

Green Chemistry

Accepted Manuscript



This article can be cited before page numbers have been issued, to do this please use: L. Fujian, C. Liu, W. Kong, C. Qi, A. Zheng and S. Dai, *Green Chem.*, 2016, DOI: 10.1039/C6GC02237E.



This is an *Accepted Manuscript*, which has been through the Royal Society of Chemistry peer review process and has been accepted for publication.

Accepted Manuscripts are published online shortly after acceptance, before technical editing, formatting and proof reading. Using this free service, authors can make their results available to the community, in citable form, before we publish the edited article. We will replace this *Accepted Manuscript* with the edited and formatted *Advance Article* as soon as it is available.

You can find more information about *Accepted Manuscripts* in the [Information for Authors](#).

Please note that technical editing may introduce minor changes to the text and/or graphics, which may alter content. The journal's standard [Terms & Conditions](#) and the [Ethical guidelines](#) still apply. In no event shall the Royal Society of Chemistry be held responsible for any errors or omissions in this *Accepted Manuscript* or any consequences arising from the use of any information it contains.



Design and synthesis of micro-meso-macroporous polymers with versatile active sites and excellent activities in production of biofuels and fine chemicals

Fujian Liu*,^{a,b} Chen Liu^a, Weiping Kong^a, Chenze Qi^a, Anmin Zheng*^d and Sheng Dai*^{b,c}Received 00th January 20xx,
Accepted 00th January 20xx

DOI: 10.1039/x0xx00000x

www.rsc.org/

Micro-meso-macroporous polymers (MOPs) grafted with versatile functional groups such as sulfonate, amine, triazole, pyridine, strong acidic ionic liquids and triphenylphosphine, were synthesized from *in-situ* cross linking of different functional molecules with 1,4-bis(chloromethyl)benzene in the presence of Lewis acids catalysts without using additional templates. The resultant hyper-cross-linked nanoporous polymers show unique characteristics such as large BET surface areas (up to 1523 m²/g), abundant micro-meso-macropores (4.5–131 nm), and tunable and versatile active sites (acid, base and palladium). These functional polymers exhibit excellent activities and good reusability in biomass conversions, cross-coupling reactions and condensation. The catalytic activities are much better than those of various conventional catalysts such as H₃PW₁₂O₄₀, SBA-15-SO₃H, Amberlyst 15, mesoporous H-ZSM-5 Pd/C and even as comparable as those of homogeneous H₂SO₄ and HCl in depolymerization of crystalline cellulose into fine chemicals and towards transesterification to biodiesel. This work highlights a low cost route to the synthesis of solid catalysts based on functional nanoporous polymers for catalyzing the production of clean biofuels and fine chemicals.

Introduction

Porous organic polymers (POPs) act as a class of *state-of-the-art* materials that have attracted extensive attentions because of their wide applications in the areas of adsorption, water treatment, gas storage and separation, and heterogeneous catalysis.^{1–13} In general, nanopores in POPs can be generated via the introduction of porogens during the curing processes. Various porogens can be used, such as SiO₂ spherical hard templates or surfactant soft templates.^{14–19} They result in the formation of controllable, ordered nanopores in polymers such as phenol-formaldehyde resin, exhibiting excellent properties in adsorption, separation and heterogeneous catalysis.^{17–21} However, the use of these nanoporous polymers in industry is limited because of the difficulty of removing the templates and the complexity of the synthetic procedures.^{16,22–24} An alternative way of synthesizing porous organic polymers, such as crystalline covalent-organic frameworks (COFs), porous polymer networks (PPNs), porous aromatic frameworks (PAFs), polymer of intrinsic microporosity (PIMs) and conjugated microporous polymers was achieved by co-condensing small-molecule building

blocks without using additional templates.^{1–11,13} The resultant microporous polymers were mainly used for gas adsorption and storage or for small-molecule catalysis.^{1–11,13,25} However, the solo microporous structures in these materials severely limit their responses to bulky molecules, which usually are present in biological systems, pharmaceutical processes, and heterogeneous catalysis.²⁶ In addition, relatively high synthetic cost also limits the synthesis of these microporous polymers on a large scale.

POPs materials with combined micro-mesopores exhibit unique characteristics such as large BET surface areas and pore volumes, enhanced accessibility of catalytically active sites, much decreased diffusion limitation for various guest molecules,^{8,9} which strongly enhance their abilities of resistance to carbon deposition and responses to bulky molecules in the area of heterogeneous catalysis.^{8,9,17–23} Notably, catalytic processes (especially biomass conversions) are very important tools for the synthesis of various useful chemicals and biofuels in industry. Recently, Xiao and coworkers have successfully synthesized a series of nanoporous polymer-based solid catalysts with adjustable nanopore sizes (3–50 nm), controllable surface wettability and active sites. They showed excellent activities and good reusability for catalyzing conversion of low cost biomass into clean biofuels and fine chemicals.^{8,9} These functional porous organic polymers were synthesized via copolymerization of divinylbenzene with functional monomers under high-temperature solvothermal conditions in the absence of any templates.^{8,9,22} However, the energy consumption of high-temperature hydrothermal or solvothermal technologies, and safety concerns associated with them, limit their use in the preparation of functional porous organic polymers with enhanced nanopore sizes in industry.²⁷

^a College of Chemistry and Chemical Engineering, Shaoxing University, Shaoxing, 312000 (China). E-mail: fjliu@usx.edu.cn.

^b Department of Chemistry, University of Tennessee, Knoxville TN 37996 (USA).

^c Chemical Sciences Division, Oak Ridge National Laboratory, Oak Ridge TN 37831 (USA). E-mail: dais@ornl.gov.

^d National Center for Magnetic Resonance in Wuhan, State Key Laboratory of Magnetic Resonance and Atomic and Molecular Physics, Wuhan Institute of Physics and Mathematics, Wuhan 430071 (China). Email: zhenqanm@wipm.ac.cn.

Electronic Supplementary Information (ESI) available: [details of any supplementary information available should be included here]. See DOI: 10.1039/x0xx00000x

Up to now, it remains a challenge to find a template free approach to synthesize porous polymer based solid catalysts with combined micro-meso-macropores, tunable and versatile functional groups under rather mild conditions.^{1,28} Herein, we report a generalized, template-free route to the synthesis of multiple groups functionalized, catalytically active micro-meso-macroporous polymers (MOPs) with abundant nanopores and tunable active sites. This route was achieved by the direct alkylation of various functional molecules with 1,4-bis(chloromethyl)benzene catalyzed by Lewis acids such as SnCl₄ and TiCl₄ under normal pressure and low temperatures. To the best of our knowledge, there is still few reports on targeted design and synthesis of micro-meso-macroporous polymers with versatile and tunable active sites. The resultant hyper-cross-linked porous polymers showed abundant micro-meso-macropores, very large BET surface areas, excellent thermal stabilities, and good wettability for various organic substrates. It is noteworthy that various functional molecules—such as resorcinol, triazole, amine, pyridine, ethylbenzene, sulfonate, imidazole, and triphenylphosphine—were directly cross-linked to produce correspondingly active nanoporous polymers. These nanoporous polymers could be used as highly efficient supports for grafting with different active sites such as sulfonic acid, strong acid ionic liquid, bases, or palladium. The resultant nanoporous polymers could be used as highly efficient and reusable solid catalysts in condensation, cross coupling reactions and biomass conversions, such as reactions toward transesterification to biodiesel, depolymerization of crystalline cellulose into fine chemicals. This work develops a facile, cost-effective approach to the synthesis of micro-meso-macroporous polymeric solid catalysts with abundant nanopores, tunable and versatile active sites, and excellent catalytic activities for catalyzing conversion of low cost biomass into renewable biofuels and useful chemicals, which are the hot topics in the area of green and sustainable chemistry.

Results and discussion

Fig. 1 and Fig. S1 show N₂ isotherms and pore size distributions of various groups of functionalized MOPs: MOP-P(Ph)₃, MOP-aniline, MOP-phloroglucinol, MOP-ethylbenzene, MOP-pyridine, MOP-triazole, and MOP-benzene. MOP-benzene exhibits a type-IV isotherm with a steep increase in adsorption at relative pressures ranging from 0.85 to 0.975, which results in hierarchical nanopore sizes centered at around 67.5 and 116.8 nm. These values indicate the formation of abundant macropores in the sample (Fig. S1 and Table 1). On the other hand, various functional groups functionalized MOPs exhibit typical type-IV isotherms with steep increases at a relative pressure of 0.4 < P/P₀ < 0.975, which results in nanopore sizes ranging from 4.5 to 31.6 nm (Fig. 1), indicating formation of abundant mesopores in these samples.^{8,9} Correspondingly, the BET surface areas and pore volumes of these samples ranged from 217 to 1523 m²/g and 0.31 to 2.86 cm³/g (Table 1), respectively. Besides mesopores, certain amounts of micropores and macropores could also be observed in these samples (Fig.1).

Notably, the volume ratios of micro/meso/macropores were distributed in the range of 1/2.7~5.7/0.2~2.7 (Table 1). These results suggest functional MOP materials with large BET surface

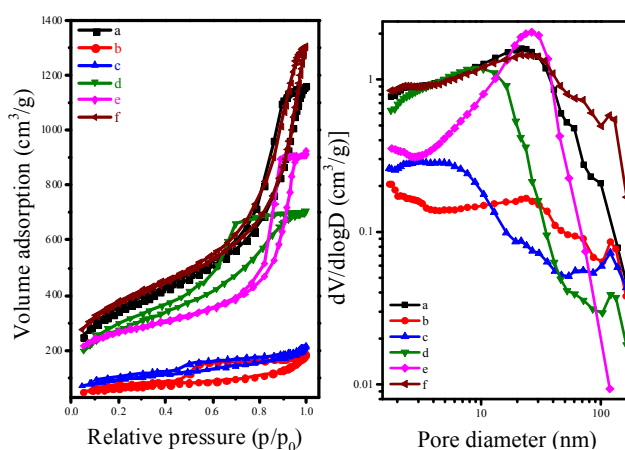


Fig. 1. N₂ adsorption-desorption isotherms and pore size distribution of (a) MOP-P(Ph)₃, (b) MOP-aniline, (c) MOP-phloroglucinol, (d) MOP-ethylbenzene, (e) MOP-pyridine, and (f) MOP-triazole.

areas and abundant micro-meso-macropores were successfully prepared in this work. The nanoporous structures, amount of

Table 1. The textural parameters and active sites contents of various samples.

Samples	Contents of active sites (mmol/g)	S _{BET} (m ² /g) ^a	V _t (cm ³ /g) ^a	Volume ratios ^e	D _p (nm) ^f
MOP-[C ₄ mim]Cl	0.14 ^b	1523	2.86	1/3.9/2.3	31.6&131
MOP-triazole	0.18 ^b	1265	1.94	1/4.5/0.9	24.3
MOP-imidazole	0.26 ^b	1238	1.96	1/4.3/1.1	16.7
MOP-P(Ph) ₃	-	1189	1.77	1/5.7/0.6	22.9
MOP-P(Ph) ₃ -Pd	1.08 ^c	987	1.62	1/4.1/1.5	21.8
MOP-ethylbenzene	-	956	1.08	1/3.9/0.3	9.6
MOP-benzene ^o	-	926	1.60	1/2.7/2.7	67.5&116.8
MOP-pyridine	2.20 ^b	868	1.27	1/4.3/0.2	26.2
MOP-ethylbenzene-SO ₃ H	1.52 ^b	580	0.78	1/3.8/0.8	7.5
MOP-benzenesulfonic acid	1.21 ^b	472	0.81	1/3.3/0.9	28.3
MOP-phloroglucinol-SO ₃ H	1.95 ^b	317	0.31	1/4.0/0.8	4.5
MOP-aniline	2.35 ^b	217	0.31	1/3.5/0.8	22.9

^a Synthesized from self cross linking of 1,4-bis(chloromethyl)benzene. ^b Nitrogen and sulfur contents were measured by elemental analysis. ^c Pd contents was measured by ICP. ^d Single point total pore volumes were calculated at the relative pressure of 0.99. ^e Volume ratios of micro/meso/macropores.

Micropore: 0–2 nm, mesopore: 2–50 nm, macropore: 50–300 nm; Micropore volume was calculated by t-plot method, mesopore and macropore volume were calculated by BJH model; ^f Pore size distribution estimated from BJH model.

micropores, mesopores and macropores may be adjusted through changing the synthetic solvents, functional molecules and their ratio to cross linker during synthetic processes.^{8,9,22} Meanwhile, the concentrations of functional groups in MOP materials ranged from 0.14 to ~2.35mmol/g (Table 1), further confirming that functional molecules with different contents were successfully grafted onto the network of MOPs. The resulting MOP materials were used as effective supports for palladium, sulfonic groups, and acidic ionic liquids, which still showed large BET surface areas and abundant nanopores (Table 1). Notably, it is possible that the loading of SO₃H groups and palladium active sites might block the nanopores and increase weight of the samples, which would partially reduce the surface areas and pore volumes of the samples (Table 1).

Fig. 2a shows scanning electron microscope (SEM) image of MOP-ethylbenzene-SO₃H, exhibiting rough surface characteristics with abundant porosities and cavities, which were distributed on the mesoporous and macroporous scales, in agreement with N₂ adsorption-desorption isotherms results; similar abundant porosities were also found in other MOPs samples (Fig. S2). Scanning transmission electron microscope (STEM) images further confirm that rough surfaces and abundant meso-macropores in MOP-ethylbenzene-SO₃H, and carbon, sulfur active sites were homogeneously dispersed in the sample. Meanwhile, MOP-P(Ph)₃-Pd also showed abundant nanopores, and C, P, and Pd with homogeneously dispersed in the sample. Similar results were found in MOP-triazole and MOP-P(Ph)₃ (Fig. S3), which confirms that various functional groups were successfully introduced into MOP-type materials. Moreover, TEM images further confirmed abundant

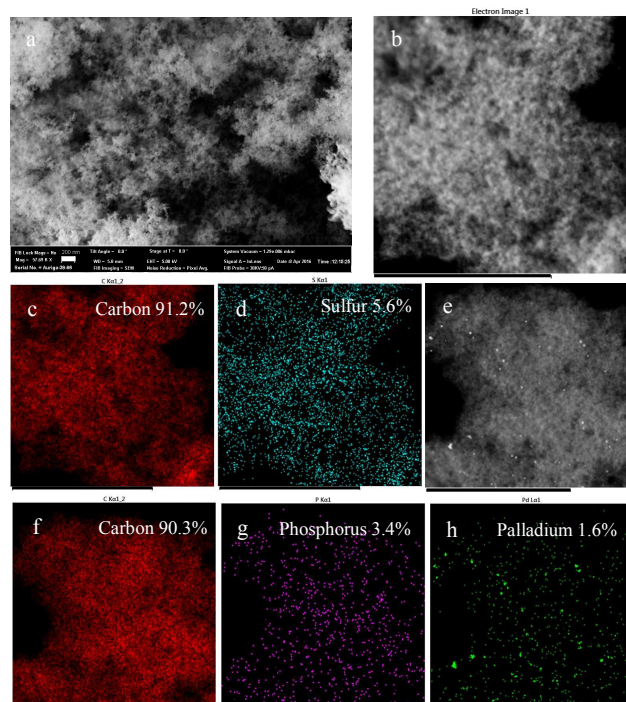


Fig. 2. (a) Scanning electron microscope (SEM) image of MOP-ethylbenzene-SO₃H. (b) Scanning transmission electron microscope (STEM) image, (c and d) element maps and contents of MOP-ethylbenzene-SO₃H. (e-h) STEM image, element maps and contents of MOP-P(Ph)₃-Pd. The scale bars of (a) is 200 nm, and (b-h) are 1 μm.

micro-meso-macropores in MOPs such as MOP-ethylbenzene-SO₃H, MOP-pyridine, MOP-P(Ph)₃-Pd, MOP-triazole, MOP-aniline, and MOP-benzene (Fig. S4). On the other hand, X-ray photoelectron spectroscopy (XPS) results further confirm that various active sites such as sulfonic acid, amine, and Pd have been successfully introduced into MOPs materials. For instance, MOP-ethylbenzene-SO₃H showed the signals of C1s, S2p, and O1s, MOP-aniline showed the signals of C1s and N1s, and MOP-P(Ph)₃-Pd showed the signals of C1s, P2p and Pd3d (Fig. S5).

Fig. 3 shows ¹³C CP/MAS nuclear magnetic resonance (NMR) spectra of MOP-P(Ph)₃, MOP-phloroglucinol, and MOP-pyridine, which were measured to reveal the cross-linked structures of the samples. Notably, the band at around 18ppm was assigned to the methyl end group in the cross-linker 1,4-bis(chloromethyl)benzene, and the bands at around 37, 42, and 45ppm were assigned to the methylene linker in the 1,4-bis(chloromethyl)benzene found in these samples, which were confined in different chemical environments. The band at 129 and 137ppm was assigned to aromatic carbon in cross-linked 1,4-bis(chloromethyl)benzene building blocks.^{18,28} For the MOP-P(Ph)₃ sample, the bands at 129

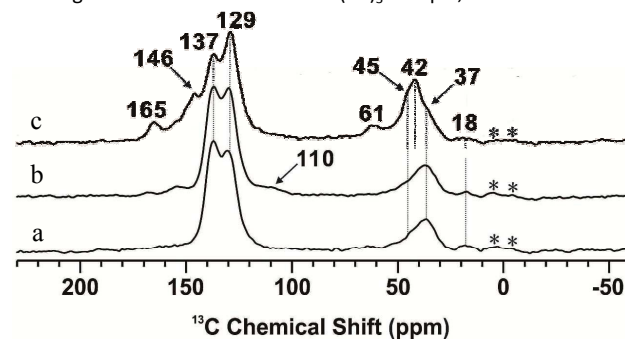


Fig. 3. ¹³C solid state nuclear magnetic resonance (NMR) spectra of (a) MOP-P(Ph)₃, (b) MOP-phloroglucinol, and (c) MOP-pyridine. Asterisks denote spinning sidebands.

and 137 ppm were assigned to aromatic carbon and unsubstituted aromatic carbon in both cross-linked 1,4-bis(chloromethyl)benzene and the P(Ph)₃ building blocks.^{18,29} On the other hand, a ³¹P solid state NMR spectrum indicated the signal of the P(Ph)₃ group with an oxidation state (Fig. S6). For MOP-phloroglucinol, the band at 110 ppm was assigned to substituted aromatic carbon in phloroglucinol; and the band at around 155 ppm was assigned to carbon atoms connected with the hydroxyl group in phloroglucinol. Similar results were also observed for MOP-pyridine, except for the characteristic peaks of the 1,4-bis(chloromethyl)benzene cross-linker. The band at 146 ppm was assigned to carbon atoms connected with nitrogen in the pyridine ring, and the band at 165 ppm was assigned to substituted carbon by the 1,4-bis(chloromethyl)benzene cross-linker in the pyridine ring. As with MOP-P(Ph)₃ and MOP-phloroglucinol, the new band at around 61 ppm was assigned to the methylene linker directly connected with nitrogen atoms in the pyridine ring. The combination of elemental analysis, XPS spectra, energy-dispersive x-ray spectroscopy, and solid state NMR results enables us to conclude that various functional groups were successfully grafted onto MOP networks via alkylation induced hyper-cross-linking of various functional

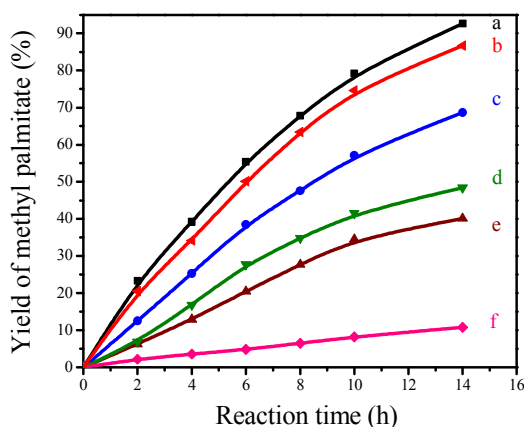
Table 2 Catalytic data in transesterification of sunflower oil with methanol over various acid catalysts^a

Catalysts	Yields of methyl esters (%)							
	Methyl palmitate (C _{16:0})	Methyl stearate (C _{18:1})	Methyl oleate (C _{18:2})	Methyl linoleate (C _{18:3})	Methyl arachidate (C _{20:0})	Methyl 11-eicosenoate (C _{20:1})	Methyl docosanoate (C _{22:0})	Methyl tetra cosanoate (C _{24:0})
MOP-aniline-[C ₄][SO ₃ CF ₃]	92.8	94.2	95.6	96.3	89.1	89.2	90.4	91.8
MOP-phloroglucinol-SO ₃ H	87.4	82.8	80.5	82.3	78.7	86.4	85.3	81.9
MOP-ethylbenzene-SO ₃ H	85.4	76.8	79.3	83.6	80.6	83.4	78.9	79.7
MOP-ethylbenzene-SO ₃ H ^b	84.5	76.3	78.6	82.7	79.2	82.5	79.2	79.1
MOP-ethylbenzene-SO ₃ H ^c	84.2	76.5	77.4	81.4	78.8	81.2	77.8	78.4
MOP-ethylbenzene-SO ₃ H ^d	83.7	76.1	77.1	79.1	78.3	81.7	78.3	77.8
MOP-ethylbenzene-SO ₃ H ^e	84.3	75.4	77.6	79.2	78.9	80.1	77.1	76.8
H ₃ PW ₁₂ O ₄₀	60.2	65.4	59.1	62.3	55.4	62.3	68.9	54.8
SBA-15-SO ₃ H	57.9	57.3	54.8	53.3	43.5	38.9	43.2	40.7
Amberlyst 15	50.7	48.2	42.6	46.5	28.3	29.8	36.5	14.2

^a 1 mL sunflower oil; 2.5 mL methanol; 0.1 g catalyst; reaction temperature 80°C; reaction time 16 h. The catalytic activity of the catalysts was characterized quantitatively by the conversion of fatty acid methyl esters (FAME, Y %) which was calculated as follows: Yield=(M₀/M_T)×100 %, where M₀ and M_T are the number of moles of each FAME produced and expected, respectively. In this section, M_T is the number of moles of FAME catalyzed by 0.1 g of H₂SO₄ in 24 h, performed at 80°C with the same content of feedstock as that of MOP solid acids. The ^b 2nd, ^c 3rd, ^d 4th and ^e 5th recycles in transesterification of sunflower oil with methanol.

molecules with 1,4-bis(chloromethyl)benzene. MOPs exhibit superior thermal stabilities, and the decomposition temperatures of both functional groups and networks in MOPs were higher than 300 and 500°C respectively (Fig. S7).

Fig. 4 shows the transesterification of tripalmitin with methanol to produce biodiesel over various catalysts. MOP-based solid acids exhibited much improved catalytic activities in comparison with H₃PW₁₂O₄₀, SBA-15-SO₃H, Amberlyst 15, and mesoporous H-ZSM-5. The yields of biodiesel (C16:0) catalyzed by MOP-aniline-[C₄][SO₃CF₃] and MOP-ethylbenzene-SO₃H were 67.9 and 63.2% after 8h of incubation, much better than the yields of heteropolyacid (47.8%), SBA-15-SO₃H (37.6%), Amberlyst 15 (29.7%) and mesoporous H-



ZSM-5 (7.8%). Further prolong the reaction time to 14 h, the yields

Fig. 4. Dependences of catalytic activities on time in transesterification of tripalmitin with methanol catalyzed by (a) MOP-aniline-[C₄][SO₃CF₃], (b) MOP-

ethylbenzene-SO₃H, (c) H₃PW₁₂O₄₀, (d) SBA-15-SO₃H, (e) Amberlyst 15, and (f) mesoporous H-ZSM-5.

of C16:0 catalyzed by MOP solid acids increased to 92.6 and 86.7%, whereas heteropolyacid, SBA-15-SO₃H, Amberlyst 15, and mesoporous H-ZSM-5 still gave relatively low yields of biodiesel at 68.6, 48.4, 40.1, and 10.9%, respectively.

Besides purified oil, MOP-based solid acids were also very active for catalyzing the conversion of sunflower oil into biodiesel; the main biodiesel products were methyl palmitate (C16:0), methyl stearate (C18:1), methyl oleate (C18:2), methyl linoleate (C18:3), methyl arachidate (C20:0), 11-eicosenoic methyl (C20:1), methyl docosanoate (C22:0), and methyl tetra cosanoate (C24:0). Notably, the yields of biodiesel [C16:0 (85.4~92.8%), C18:1 (76.8~94.2%), C18:2 (79.3~95.6%), C18:3 (82.3~96.3%), C20:0 (78.7~89.1%), C20:1 (83.4~89.2%), C22:0 (78.9~90.4%) and C24:0 (79.7~91.8%)] catalyzed by MOP-phloroglucinol-SO₃H, MOP-ethylbenzene-SO₃H, and MOP-aniline-[C₄][SO₃CF₃] were much higher than the yields of H₃PW₁₂O₄₀, Amberlyst-15, and SBA-15-SO₃H (as presented in Table 2). Compared with sulfonic group grafted MOPs, the enhanced activity of MOP-aniline-[C₄][SO₃CF₃] should be attributed to its unique strong ionic liquid active site, which was very active for catalyzing biomass conversions.^{9,22} In addition, MOPs solid acids showed very good recyclability, and no obvious decrease was seen in biodiesel yields catalyzed by MOP-ethylbenzene-SO₃H recycled for five times (Table 2). The excellent catalytic activities and good reusability found in MOP-based solid acids can be attributed to their large BET surface areas, abundant nanopores, good stabilities, strong and tunable acid sites. Abundant nanopores could strongly enhance the mass transfer during various

Table 3 Yields of sugars and dehydration products in the depolymerization of Avicel catalyzed by various solid acids ^a.

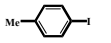
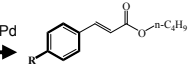
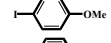
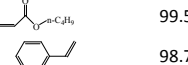
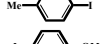
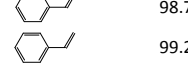
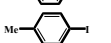
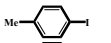
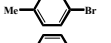
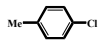
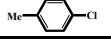
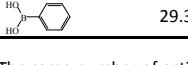
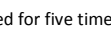
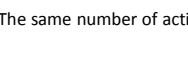
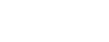
Samples	Glucose yield (%) ^b	Cellobiose yield (%) ^b	HMF yield (%) ^b	TRS (%) ^c
Amberlyst 15	15.2	16.8	2.9	39.7
HCl ^d	40.7	26.3	9.8	85.6
MOP-ethylbenzene-SO ₃ H	38.8	27.1	8.9	83.7
MOP-aniline-[C ₄][SO ₃ CF ₃]	42.6	32.9	10.3	90.4

^a0.1g of Avicel, 1.5g of [C₄mim]Cl ionic liquid, and 0.5mL of DMSO mixed solvents, 20mg of catalyst; the reaction was performed at 100°C for 5h. ^b Measured by HPLC method. ^c Measured by DNS method. ^d The same number of acidic sites as in MOP-ethylbenzene-SO₃H.

catalytic reactions, strong and tunable acid sites could effectively activate reactants. The above characteristics result in the synergistic effect, which leads to the higher catalytic performances of the MOP-based catalysts.

We further investigated the catalytic performances of MOP-based solid acids in the depolymerization of crystalline cellulose into sugars and hydroxymethylfurfural (HMF), which is thought to

Table 4 Catalytic data of MOP-P(Ph)₃-Pd solid catalyst in Heck and Suzuki cross-coupling reactions with different substrates.

Samples	Substrate 1	Substrate 2	Yields (%)
MOP-P(Ph) ₃ -Pd			99.8
MOP-P(Ph) ₃ -Pd			99.5
MOP-P(Ph) ₃ -Pd			98.7
MOP-P(Ph) ₃ -Pd			99.2
MOP-P(Ph) ₃ -Pd			~100
MOP-P(Ph) ₃ -Pd ^a			99.2
Palladium acetate ^b			99.6
MOP-aniline-Pd			96.5
MOP-P(Ph) ₃ -Pd			98.3
MOP-P(Ph) ₃ -Pd			68.5
Palladium acetate ^b			29.3

^aThe sample has been recycled for five times. ^b The same number of active site as that of MOP-P(Ph)₃-Pd.

be a green, low-cost way of transforming biomass into important intermediates and useful chemicals. Notably, the catalytic activities of MOP-ethylbenzene-SO₃H and MOP-aniline-[C₄][SO₃CF₃] were much better than those of Amberlyst 15 and even homogeneous HCl catalysts (Table 3). For example, the total reduced sugar (TRS) values of MOP-ethylbenzene-SO₃H and MOP-aniline-[C₄][SO₃CF₃] were 83.7 and 90.4%, and the TRS value of HCl was 85.6%. On the other hand, the TRS value of Amberlyst 15 was as low as 39.7%. The main products were glucose, fructose, and HMF; and the yields of those products catalyzed by MOP solid acids were higher than yields catalyzed by HCl and much higher than those catalyzed by Amberlyst 15 (Table 3).

MOPs could also be used as efficient support for loading with palladium, which are still used as highly efficient and reusable catalysts in cross-coupling reactions (Table 4). Cross coupling reactions such as Suzuki and Heck reactions could be acted as an effective tool for the synthesis of useful chemicals in the areas of pharmaceutical process and organic synthesis. Notably, MOP-P(Ph)₃-Pd was very active in these reactions. When iodobenzene was employed as substrate, the yields of products was nearly 100% within 1h, even after being recycled for 5 times, MOP-P(Ph)₃-Pd still exhibited excellent activity, giving the products yield at 99.2%. Similar high activity in MOP-P(Ph)₃-Pd could also be found in Heck reaction, in the reactions of iodobenzene with styrene and n-butyl acrylate, the yields of products were up to 99.8 and 98.7%, respectively. Except for iodobenzene, MOP-P(Ph)₃-Pd was also very active for catalyzing cross coupling of bromobenzene, after 5h reaction, the yields of products in Heck and Suzuki coupling reactions were 96.5 and 98.3%, respectively. Further expand the substrate to chlorobenzene, MOP-P(Ph)₃-Pd still gives relative high product yield as high as 68.5%.

Furthermore, MOPs could also be grafted with basic sites such as amine and pyridine, which still can be used as highly efficient and reusable nanoporous solid bases in Knoevenagel condensation. The activities of MOP solid base were much better than that of basic resin of Amberlite 400 (As presented in Table 5). For instance, in the reaction of benzaldehyde with malononitrile, the yield of the

Table 5 The catalytic activities in Knoevenagel condensation over various samples.

Catalysts	Substrates	Products	Yields (%)
MOP-Pyridine			>99.5
MOP-Aniline			>99.5
MOP-Pyridine			98.5
MOP-Aniline			97.8
Amberlite 400-OH			64.6
MOP-Aniline ^a			99.1

^aThe 5th recycles in Knoevenagel condensation of benzaldehyde with malononitrile.

product catalyzed by MOP-Pyridine and MOP-Aniline were higher than 99.5% for 1h reaction, while Amberlite-400 gave very low yield at 64.6%. In addition, even after being recycled for 5 times, MOP-aniline still gave the product yield as high as 99.1%, indicating its very good reusability. Similar results could also be observed in other substrate such as salicylaldehyde (Table 5). The excellent catalytic activities found in MOPs solid catalysts are attributable to their large BET surface areas, abundant micro-meso-macropores, controllable surface wettability, tunable and homogeneous dispersion of active centers, which strongly enhance accessibility of active sites to various substrates. This work develops an efficient and generalized approach to targeted synthesis of multifunctional porous polymers based solid catalysts that offer great opportunity for wide application of MOPs to catalyze the production of biofuels and fine chemicals with different molecule sizes.

Conclusions

In summary, this work develops a facile, generalized approach to the targeted synthesis of the micro-meso-macroporous polymers functionalized with various functional groups, which was achieved via one-step alkylation of functional small molecules with 1,4-bis(chloromethyl)benzene without using organic templates. MOPs have large BET surface areas, abundant micro-meso-macropores, tunable and versatile active sites. The above characteristics result in their excellent activities and reusabilities for catalyzing conversion of low cost biomass into green and renewable biofuels and fine chemicals, which are very important for their wide applications in the areas of green and sustainable chemistry.

Acknowledgements

FL and AZ was supported by the National Natural Science Foundation of China (21573150, 21203122, 21522310, 21473244), and the Natural Science Foundation of Zhejiang Province (LY15B030002). SD was supported by the Division of Chemical Sciences, Geosciences and Biosciences, Office of Basic Energy Sciences, U.S. Department of Energy.

Experimental

Chemical and reagents

All reagents were of analytical grade and used as purchased without further purification. Microcrystalline cellulose (Avicel), 1-n-butyl-3-methylimidazolium ([C₄mim]Cl), phloroglucinol, triazole, aniline, pyridine, 1,4-bis(chloromethyl)benzene, ethylbenzene, *p*-styrene sulfonate, imidazole, triphenylphosphine, palladium acetate, and tripalmitin were purchased from Sigma-Aldrich Co. Dichloroethane, SnCl₄, TiCl₄, ethanol, THF, iodobenzene, *n*-butyl acrylate, salicylaldehyde, benzaldehyde, malononitrile, styrene, dichloromethane, *N,N*-Dimethylformamide (DMF), 1,3-propanesultone, HCl, HSO₃Cl, H₂SO₄, DMSO, ethanol,

methanol, sunflower oil, dodecane were obtained from Sinopharm Chemical Reagents Co. Ltd.

Synthesis of samples

MOPs were synthesized by the alkylation cross-linking of different functional molecules with 1,4-bis(chloromethyl)benzene. In a typical run for the synthesis of triphenylphosphine functionalized nanoporous polymers, 1.0g of 1,4-bis(chloromethyl)benzene was dispersed into 15 mL of 1,2-dichloroethane solvent, followed by the addition of 3 mL of SnCl₄ or TiCl₄ at 0°C under vigorous stirring. Then, 0.8 g of triphenylphosphine was added into the mixture, and alkylation was performed at 65–75°C for 24h under an insert gas. The resulting hyper-cross-linked sample was washed with a hot ethanol–HCl mixed solution several times to remove the Lewis acid catalysts and then dried under vacuum at 60°C for 24h. The final samples were denoted as MOP-P(Ph)₃. Other functional groups can be introduced into MOPs via a similar procedure. After good dispersion of 1,4-bis(chloromethyl)benzene and SnCl₄ into a 1,2-dichloroethane solvent, a certain content of functional small molecules—such as phloroglucinol, triazole, aniline, pyridine, ethylbenzene, *p*-styrene sulfonate, imidazole, and [C₄mim]Cl—were added into the mixture; and alkylation-induced cross-linking was accomplished by heating the mixture at 65–75°C for 24h. Self cross-linking of 1,4-bis(chloromethyl)benzene can also be accomplished using similar procedures without adding other functional molecules, which results in MOPs with pure benzene networks. Typically, 1.8g of 1,4-bis(chloromethyl)benzene was dispersed into 15mL of 1,2-dichloroethane solvent, followed by the addition of 3mL of SnCl₄ or TiCl₄ as the catalyst at 0°C under vigorous stirring. Then self-alkylation of 1,4-bis(chloromethyl)benzene was performed at 65–75°C for 24h. The resulting hierarchical nanoporous polymer was obtained by washing with an abundant amount of a hot ethanol–HCl mixed solution several times, and drying under vacuum at 60°C for 24h. The sample was designated as MOP-benzene.

Palladium-loaded MOPs were synthesized by stirring nanoporous polymers into a solution containing methanol and weight-quantitative palladium acetate, based on the unique interactions between palladium species and functional groups in MOPs. As a typical run for synthesis of MOP-P(Ph)₃-Pd, 1.0g of MOP-P(Ph)₃ was added into a solution containing 40mL of methanol and 0.01g of palladium acetate. After the mixture was stirred for 12h under refluxing (65°C), MOP-P(Ph)₃-Pd was obtained via vacuum distillation at 45°C to remove the solvent, washing with a large amount of dimethyl ether, and drying at 60°C for 12h. In addition, other nitrogen-doped MOPs, such as MOP-pyridine and MOP-imidazole, were used as effective supports for loading with palladium species. In comparison, palladium-loaded ordered mesoporous silica (SBA-15-Pd) and activated carbon (activated carbon-Pd) were synthesized by similar procedures to that used for MOP-P(Ph)₃-Pd.

Sulfonic groups functionalized MOP could be synthesized from sulfonation of MOP supports with HSO₃Cl in presence of

dichloromethane solvent at 0°C; Typically, 1.0g of MOP samples was added into a mixture contains 40mL dichloromethane and 8mL HSO₃Cl, after stirring of the mixture at 0°C for 24h, the reaction mixture was dispersed into 300mL of water. Finally, the product was obtained from filtering, washing with a large amount of water until neutral, stirring in dioxane, and drying at 80°C. MOP-benzene, MOP-phloroglucinol and MOP-ethylbenzene could be used as suitable supports for grafting with sulfonic group.

Sulfonic group functionalized MOP can also be synthesized from cross linking of sodium benzenesulfonate by using 1,4-bis(chloromethyl)benzene. Typically, certain contents of 1,4-bis(chloromethyl)benzene and SnCl₄ were dissolved into 1,2-dichloroethane solvent, then sodium benzenesulfonate functional molecules were added into the mixture, the alkylation cross linking was performed at 65-75°C for 24h under vigorous stirring. The resultant solid product could be obtained from washing with abundant hot ethanol-HCl mixed solution for several times, and dried under vacuum condition at 60°C for 24h to gave sulfonic group functionalized nanoporous polymers. To adjust concentrations of sulfonic groups, different contents of sodium benzenesulfonate was added in the initially synthetic process.

Strong acid ionic liquid groups can also be grafted onto the networks of MOPs. Typically, 1.0g of MOP-aniline or MOP-pyridine were added into a mixture contains 0.3g of 1,4-butanediol and 25mL of toluene, then the reaction temperature was increased up to 100°C and kept at 100°C for 12h. After cooling to room temperature, 2.5mL of HSO₃CF₃ was introduced, after stirring of the mixture for 24h at room temperature. The sample could be collected from filtration, washing with abundant CH₂Cl₂-ethanol mixed solvents for removing of residual HSO₃CF₃, and drying at 80°C under vacuum condition. MOP-aniline-[C₄][SO₃CF₃] or MOP-pyridine-[C₄][SO₃CF₃] were obtained (Where C₄ stands for 1,4-butanediol and SO₃CF₃ stands for the anion exchanged acid of HSO₃CF₃). The above acidification methods result in the samples functionalized with typical Bronsted acid sites.^{9,22,23}

Characterizations

Nitrogen isotherms of the samples at -196°C were measured using a Micromeritics ASAP 2020 M system. The samples were outgassed for 6h at 200°C before measurements, the pore-size distribution of nanopores in the sample was calculated by using the Barrett-Joyner-Halenda (BJH) model. Thermogravimetric analyses (TG) were performed on a Perkin-Elmer TGA7 in flowing air with a heating rate of 20°C/min. The acid exchange capacities of the catalysts were determined by acid-base titration with standard NaOH solution. XPS spectra were performed on a Thermo ESCALAB 250 with Al K α radiation, and binding energies were calibrated using the C1s peak at 284.9eV. CHNS elemental analysis was performed on a Perkin-Elmer series II CHNS analyzer 2400. TEM images were performed on a FEI Tecnai G2 F20 s-twin D573 transmission electron microscope working at 200kV. SEM results were performed on a Zeiss

Auriga Crossbeam field emission scanning electron microscope at an acceleration voltage of 5kV. The ¹³C solid state NMR experiments were carried out on a Varian Infinityplus-300 spectrometer at resonance frequencies of 299.78 and 75.38MHz for ¹H and ¹³C, respectively. The experiments were recorded using a 4mm double-resonance MAS probe at a spinning rate of 10 kHz. Pulse width ($\pi/2$) for ¹³C was measured to be 4.1 μ s. A contact time of 4 ms and a recycle delay of 3s were used for the ¹H-¹³C CP/MAS measurement. The chemical shift of ¹³C was externally referenced to hexamethylbenzene.

Catalytic reactions

Suzuki reaction

0.25mmol of 4-iodotoluene, 0.375mmol of aryl boronic acids, and 0.5mmol of K₂CO₃ were mixed into a flask, followed by addition of 10mg of MOP-P(Ph)₃-Pd (10mg, 1.0wt% of palladium acetate) catalyst, subsequently, 3.0mL of EtOH and 1.0mL of H₂O was also introduced as the solvents. The reaction mixture was heated at 80°C for 30min under refluxing condition. When 4-bromotoluene was employed as substrate, 0.25mmol of 4-bromotoluene, 0.375mmol of aryl boronic acids, and 0.5mmol of K₂CO₃ were mixed into a flask, followed by addition of 10 mg of MOP-P(Ph)₃-Pd (10mg, 1.0wt% of palladium acetate) catalyst, subsequently, 3.0 mL of DMF and 1.0mL of H₂O was also introduced as the solvents. The reaction mixture was performed at 120°C for 5h. When 4-chlorotoluene was employed as substrate, 0.25mmol of 4-chlorotoluene, 0.375mmol of aryl boronic acids, and 0.5mmol of K₂CO₃ were mixed into a flask, followed by addition of 10 mg of MOP-P(Ph)₃-Pd (10mg, 1.0wt% of palladium acetate) catalyst, subsequently, 4.0mL of DMF was also introduced as the solvents. The reaction mixture was performed at 120°C for 7h. In these reactions, 1mmol of dodecane as internal standard was also introduced into the reaction mixture, and the GC yields of various products were analyzed by gas chromatography of Agilent 7890.

Heck reaction

1mmol of aromatic halide, 2mmol of alkenes, MOP-P(Ph)₃-Pd catalyst (2 μ mol Pd) and 3mmol of potassium acetate was dispersed into 3mL of DMSO solvent into a three-necked flask equipped with a condenser and a magnetic stirrer. Then, the reaction mixture was heated up to 110°C and lasted for 5h, after cooling to room temperature, the reaction mixture was diluted with acetone, filtered and analyzed by gas chromatography of Agilent 7890 to give the GC yields of various products. In this reaction, 1mmol of dodecane as internal standard was also introduced into the reaction mixture.

Knoevenagel condensation

Knoevenagel condensation of aldehydes with malononitrile was performed at 80°C catalyzed by MOP-Aniline and MOP-

Pyridine solid bases. Typically, 2mmol of aldehydes (benzaldehyde, salicylaldehyde), 0.02g of catalyst and 2mmol of malononitrile were mixed well into 5mL of ethanol solvent, then the reaction temperature was rapidly increased up to 80°C, the reaction was lasted for 1h. The products were analyzed by using gas chromatography systems (Agilent 7890) with a flame ionization detector (FID). The yields of products were calculated through the internal standard (dodecane) method. In addition, the catalysts could be regenerated from centrifugation, washing with abundant ethanol and drying at 60°C. The regenerated catalyst was used directly for the next run.

Transesterifications

Transesterification of tripalmitin with methanol was performed as follows: 0.84g (1.04mmol) of tripalmitin was added into a three-necked round flask equipped with a condenser and a magnetic stirrer, then the reacted temperature was rapidly increased to 65°C. After tripalmitin melting, 2.47mL (61mmol) of methanol and 0.1g of catalyst was quickly added under vigorous stirring, the reaction was lasted for 14h at 65°C. The molar ratio of tripalmitin/methanol was 1/58.7 and the mass ratio of catalyst/tripalmitin was 0.119. The product was methyl palmitate with selectivity near 100%. For products analysis, 0.5mL of the reaction mixture was firstly dispersed into 5mL of acetone, filtered and analyzed by gas chromatography of Agilent 7890. The column was HP-INNOWax capillary column (30m); the initial temperature was 100°C with the ramping rate of 20°C/min, and final temperature was 280°C; the temperature of FID detector was 300°C and dodecane was used as internal standard.

Transesterification of sunflower oil with methanol was performed as follows: 1.0g of sunflower oil (1.16mmol) was added into a three-necked round flask equipped with a condenser and a magnetic stirrer, and the temperature was increased to 65°C. Then, 3.5mL of methanol (86.3mmol) and 0.1g of catalyst were quickly added under vigorous stirring, the reaction was lasted for 18h. The molar ratio of sunflower oil/methanol was 1/72.1 and the mass ratio of catalyst/sunflower oil was 0.1. The main products were methyl palmitate (C16:0), methyl stearate (C18:1), methyl oleate (C18:2), methyl linoleate (C18:3), methyl arachidate (C20:0), 11-eicosenoic methyl (C20:1), methyl docosanoate (C22:0) and methyl tetracosanoate (C24:0), the quantitative analysis was performed by using Agilent GC/MS instrument (Agilent 6890N/5975I) with a programmable split/splitless injector. The injector-port temperature was set at 270°C. The oven-temperature program was initially set at 140°C and ramped to 270°C with the ramping rate of 10°C/min.

Depolymerization of microcrystalline cellulose

Catalyze depolymerization of microcrystalline cellulose of Avicel was chosen as the model reaction for evaluating the activities of nanoporous polymeric solid acids. Typically, 100 mg of Avicel was dissolved into a mixture contains 1.5g of

[C₄mim]Cl ionic liquid and 0.5mL of DMSO, which was basically dissolved after vigorous stirring at 100°C for 3-5h, then 20mg of MOP-ethylbenzene-SO₃H solid acid was added. After that, 600μL of water acted as reactant was slowly introduced into the reaction mixture. At different time intervals, the reaction mixture was withdrawn, weighed, quenched immediately with cold water, and centrifuged at 14,800rpm for 5min to separate unreacted cellulose. For comparison, Amberlyst 15 and HCl were also used as catalysts for catalyzing depolymerization of Avicel, which were performed with similar procedures as that of MOP-ethylbenzene-SO₃H. Notably, the isolated crystalline cellulose was thoroughly washed with water, and recovered through centrifugation. The amount of isolated cellulose could be determined by weighing.

Total Reducing Sugar (TRS)

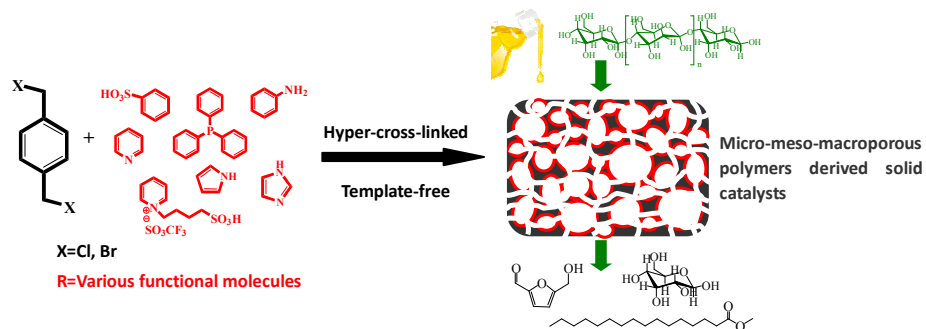
In this work, TRS method was thought to be a reliable technology to evaluate depolymerization degree of crystalline cellulose, which was tested via DNS method³⁰⁻³². Typically, a mixture contains 0.5mL of 3,5-dinitrosalicylic acid (DNS) reagent and 0.5mL of isolated reaction mixture was heated for 5min at 100°C. Then, the mixture was diluted by using 4mL of deionized water. The color changes of the mixture were measured in a NanoDrop 2000 UV-spectrophotometer at the wave length of 540nm. The concentrations of the total reducing sugars was calculated based on a standard curves.

In this reaction, the concentrations of the products such as glucose, cellobiose and HMF were measured by the Shimadzu LC-20A HPLC system based on standard curve method, which was equipped with a SCR-101N column using extra-pure water as mobile phase with a flow rate of 0.5mL/min. The column's temperature was set to 50°C. In the meantime, a refraction index was used for detection of sugars in the water. The UV detector with wavelength number at 254nm was used for detection of 5-hydroxymethylfurfural (HMF) based on standard curve method, which was equipped with a CAPCELL PAK C18 column using methanol and water (methanol/water=80:20) as mobile phase, at a flow rate of 0.7mL/min and the column's temperature was set at 50°C.

Notes and references

- 1 D. Wu, F. Xu, B. Sun, R. Fu, H. He and K. Matyjaszewski, *Chem. Rev.* 2012, **112**, 3959–4015.
- 2 O. M. Yaghi, M. O'Keeffe, N. W. Ockwig, H. K. Chae and M. Eddaoudi, J. Kim, *Nature*, 2003, **423**, 705–714.
- 3 S. S. Han, H. Furukawa, O. M. Yaghi and W. A. Goddard, *J. Am. Chem. Soc.*, 2008, **130**, 11580–11581.
- 4 A. P. Côté, A. I. Benin, N. W. Ockwig, M. O'Keeffe, A. J. Matzger and O. M. Yaghi, *Science*, 2005, **310**, 1166–1170.
- 5 S.-Y. Ding, J. Gao, Q. Wang, Y. Zhang, W.-G. Song, C.-Y. Su and W. Wang, *J. Am. Chem. Soc.*, 2011, **133**, 19816–19822.
- 6 M. G. Schwab, B. Fassbender, H. W. Spiess, A. Thomas, X. L. Feng and K. Müllen, *J. Am. Chem. Soc.*, 2009, **131**, 7216–7217.
- 7 J. Schmidt, J. Weber, J. D. Epping, M. Antonietti and A. Thomas, *Adv. Mater.*, 2009, **21**, 702–705.
- 8 Q. Sun, Z. F. Dai, X. J. Meng and F.-S. Xiao, *Chem. Soc. Rev.*, 2015, **44**, 6018–6034.

- 9 F. J. Liu, L. Wang, Q. Sun, L. F. Zhu, X. J. Meng and F.-S. Xiao, *J. Am. Chem. Soc.*, 2012, **134**, 16948–16950.
- 10 H. Furukawa and O. M. Yaghi, *J. Am. Chem. Soc.*, 2009, **131**, 8875–8883.
- 11 T. Ben, H. Ren, S. Q. Ma, D. P. Cao, J. H. Lan, X. F. Jing, W. C. Wang, J. Xu, F. Deng, J. M. Simmons, S. L. Qiu and G. S. Zhu, *Angew. Chem. Int. Ed.*, 2009, **48**, 9457–9460.
- 12 J. S. Zhang, Z.-A. Qiao, S. M. Mahurin, X. G. Jiang, S.-H. Chai, H. F. Lu, K. Nelson and S. Dai, *Angew. Chem. Int. Ed.*, 2015, **54**, 4582–4586.
- 13 S. Y. Ding and W. Wang, *Chem. Soc. Rev.*, 2013, **42**, 548–568.
- 14 E. C. Peters, F. Svec and J. M. J. Frechet, *Adv. Mater.*, 1999, **11**, 1169–1181.
- 15 H. Yokoyama, L. Li, T. Nemoto and K. Sugiyama, *Adv. Mater.*, 2004, **16**, 1542–1546.
- 16 S. A. Johnson, P. J. Ollivier and T. E. Mallouk, *Science*, 1999, **283**, 963–965.
- 17 F. Q. Zhang, Y. Meng, D. Gu, Y. Yan, C. Z. Yu, B. Tu and D. Y. Zhao, *J. Am. Chem. Soc.*, 2005, **127**, 13508–13509.
- 18 Y. Meng, D. Gu, F. Q. Zhang, Y. F. Shi, H. F. Yang, Z. Li, C. Z. Yu, B. Tu and D. Y. Zhao, *Angew. Chem., Int. Ed.*, 2005, **44**, 7053–7059.
- 19 C. D. Liang and S. Dai, *J. Am. Chem. Soc.*, 2006, **128**, 5316–5317.
- 20 Y. Wan, H. Y. Wang, Q. F. Zhang, M. Klingstedt, O. Terasaki and D. Y. Zhao, *J. Am. Chem. Soc.*, 2009, **131**, 4541–4550.
- 21 R. Xing, N. Liu, Y. M. Liu, H. H. Wu, Y. W. Jiang, L. Chen, M. Y. He and P. Wu, *Adv. Funct. Mater.*, 2007, **17**, 2455–2461.
- 22 F. J. Liu, R. K. Kamat, I. Noshadi, D. Peck, R. S. Parnas, A. M. Zheng, C. Z. Qi and Y. Lin, *Chem. Commun.*, 2013, **49**, 8456–8458.
- 23 F. J. Liu, X. J. Meng, Y. L. Zhan, L. M. Ren, F. Nawaz and F. S. Xiao, *J. Catal.*, 2010, **271**, 52–58.
- 24 A. Zalusky, O. V. Roberto, J. H. Wolf and M. A. Hillmyer, *J. Am. Chem. Soc.*, 2002, **124**, 12761–12773.
- 25 Q. H. Yang, Q. Xu, S.-H. Yu and H.-L. Jiang, *Angew. Chem. Int. Ed.*, 2016, **55**, 3685–3689.
- 26 U. Díaz and A. Corma, *Coordination Chem. Rev.*, 2016, **311**, 85–124.
- 27 R. E. Morris and S. L. James, *Angew. Chem. Int. Ed.*, 2013, **52**, 2163–2165.
- 28 Y. Wan and D. Y. Zhao, *Chem. Rev.*, 2007, **107**, 2821–2860.
- 29 Z.-A. Qiao, S.-H. Chai, K. Nelson, Z. H. Bi, J. H. Chen, S. M. Mahurin, X. Zhu and S. Dai, *Nat. Comm.*, 2014, **5**, 3705–3712.
- 30 R. Rinaldi and F. Schüth, *ChemSusChem*, 2009, **2**, 1096–1107.
- 31 R. Rinaldi, R. Palkovits and F. Schüth, *Angew. Chem. Int. Ed.*, 2008, **47**, 8047–8050.
- 32 C. Z. Li and Z. K. Zhao, *Adv. Synth. Catal.*, 2007, **349**, 1847–1850.



Micro-meso-macroporous polymeric solid catalysts with versatile active sites were synthesized from hyper-cross-linking of various functional molecules, which exhibit excellent catalytic activities for biofuels production and fine chemicals synthesis.